Modeling the relaxation of early VLF perturbations associated with transient luminous events

Christos Haldoupis,[1] Ágnes Mika,[2] and Sergey Shalimov[3]

Received 30 March 2009; revised 18 June 2009; accepted 15 July 2009; published 17 October 2009.

[1] Studies show that early VLF perturbations, characterized by abrupt signal onsets and long recoveries, occur often in relation with transient luminous events, especially sprites and sprite halos. Also, most of the early VLF events are attributed to forward scattering of subionospheric VLF transmissions incident upon horizontally elongated disturbances of elevated ionization in the upper D region. This concept is supported by the similarity of early VLF event recoveries to those of lightning-induced electron precipitation events (LEPs), which are due to electron density enhancements in the upper D region caused by lightning and whistler-induced precipitation of radiation belt electrons. Here, the simplified Glukhov-Pasko-Inan model, that has been developed for LEP investigations, is applied to simulate early VLF event recoveries observed simultaneously with sprite discharges in the D region. The present study shows that: (1) early VLF events with longer (shorter) recoveries are likely to come from higher altitudes of about 80–90 km (lower altitudes of about 70–80 km) and under conditions of lower (higher) electron density elevations relative to ambient values; (2) although negative ion and positive cluster ion production plays a role in electron density relaxation at lower heights, the electron–single ion dissociative recombination is likely the key process at upper D region heights that defines the relaxation of early VLF perturbations; and (3) tentative estimates of electron density increases responsible for early VLF events may reach values possibly higher than 10^4 electrons per cm^3 in the upper D region ionosphere.

Citation: Haldoupis, C., Á. Mika, and S. Shalimov (2009), Modeling the relaxation of early VLF perturbations associated with transient luminous events, *J. Geophys. Res.*, *114*, A00E04, doi:10.1029/2009JA014313.

1. Introduction

[2] The "early VLF events" represent a distinct category of short timescale perturbations observed in VLF transmissions propagating in the earth-ionosphere waveguide [e.g., see *Rodger*, 2003, and references therein]. They are attributed to conductivity modifications in the lower ionosphere caused by thunderstorm lightning effects. Their nature is signified by the word "early," meaning they occur right after a lightning discharge which implies a direct energetic coupling process between lightning in the troposphere and the lower ionosphere. The term "early/fast" used widely in the past to identify these phenomena is not used here because it may not be always representative. As shown by *Haldoupis et al.* [2006], the property "fast," which is meant to describe rapid onset durations of less than ~20 ms, does not apply for many early VLF events which exhibit much larger onset durations reaching values up to ~2.5 s.

[3] Early VLF events have been studied in the last several years, mostly at Stanford University [e.g., see *Inan et al.*, 1995; *Johnson and Inan*, 2000; *Barrington-Leigh et al.*, 2001; *Moore et al.*, 2003; *Marshall et al.*, 2006] (and several more papers), the University of Otago [e.g., see *Dowden et al.*, 1996; *Rodger*, 2003, and references therein], and recently the University of Crete (e.g., see overview paper on the Crete studies by *Mika and Haldoupis* [2008]). These studies established that early VLF events occur often in close association with "transient luminous events" (TLEs), particularly sprites and halos [e.g., see *Moore et al.*, 2003; *Haldoupis et al.*, 2004; *Mika et al.*, 2005; *Marshall et al.*, 2006], and occasionally also with elves [*Mika et al.*, 2006]. Most of the early event onsets coincide with sprites which are known to require a causative positive cloud-to-ground (+CG) discharge of a large charge moment change [e.g., see *Cummer and Lyons*, 2005]. Figure 1 shows a typical early VLF event observed concurrently with a sprite during the 2003 EuroSprite campaign [*Neubert et al.*, 2005]. The figure is provided here for the reader to visualize the early VLF signature, which is characterized by an abrupt onset and a signal recovery ranging typically from several seconds to several tens of seconds.

[4] There is evidence to suggest that sprite-related early events are due to forward scattering of VLF waves from regions of perturbed conductivity caused by electron density enhancements in the upper D region (e.g., see *Haldoupis et al.* [2006, and references therein] for a detailed discussion). This agrees with the fact that D region conductivity pertur-

[1]Physics Department, University of Crete, Heraklion, Crete, Greece.
[2]BMT ARGOSS B.V., Marknesse, Netherlands.
[3]Institute of Physics of the Earth, and Space Research Institute, Moscow, Russia.

0148-0227/09/2009JA014313$09.00

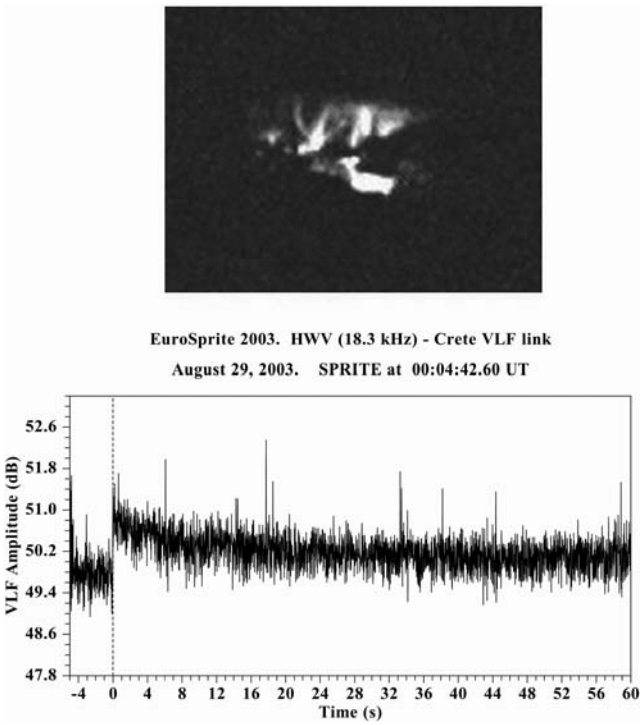

Figure 1. A typical example of an early VLF event associated with a sprite observed during the 2003 EuroSprite campaign. Typically, early event recoveries range from about 10 s to more than 200 s and are comparable to those observed in LEP perturbations.

bations on timescales larger than a second are determined solely by changes in electron density. Further, telescopic imaging of sprite displays [e.g., see *Gerken and Inan*, 2000] shows that these are characterized by a lower (50–70 km) streamer-like region, and often, but not always, by a higher (70–90 km) region of a laterally extended glow. Model estimates of electron density elevations produced in the upper regions of sprite breakdown and/or sprite halos led *Barrington-Leigh et al.* [2001] to suggest that those are likely responsible for most of the early events seen in VLF transmissions. This conclusion, which is in line with the findings of *Johnson et al.* [1999] on the horizontal extent of the perturbed conductivity regions, the quasi-electrostatic (QE) field theory of *Pasko et al.* [1997] on sprite generation and ionization production, and the theory of *Poulsen et al.* [1993] on VLF wave scattering from elongated volumes of electron density enhancements in the upper D region, was verified approximately by *Moore et al.* [2003]. These authors used a model of VLF propagation and scattering in the earth-ionosphere waveguide to reproduce, although with some uncertainty in amplitude, early VLF perturbations by taking horizontally elongated volumes of elevated electron density situated in the upper D region between 70 and 90 km.

[5] It is important to stress that the present study does not deal with early VLF perturbations not accompanied by TLEs. Such events have been attributed by *Marshall et al.* [2008] to lightning electromagnetic pulse-driven dissociative electron attachment that leads to electron density depletions which are confined at lower D region heights.

[6] In the present study, early VLF events are assumed to be caused by forward scattering from areas of enhanced conductivity (or electron density) in the upper D region. This conviction is reinforced by the fact that the early event signal recoveries are comparable to those of LEP events, referring to Lightning-induced radiation belt Electron Precipitation occurrences [e.g., see *Voss et al.*, 1984; *Inan and Carpenter*, 1987; *Rodger*, 2003; *Peter and Inan*, 2005, and references therein]. LEPs have onsets which are delayed by ~0.5 to 1.5 s relative to their causative CG lightning discharges, which distinguishes them from early events in the VLF recordings. Other than the onset delay, both LEP and early events look fairly similar in narrowband VLF recordings, particularly with respect to their recoveries.

[7] The similarity between the relaxation times of early and LEP perturbations offered the motivation to apply here for the early events the same D region model used in LEP investigations. This, which in the following is referred to as Glukhov-Pasko-Inan (GPI) model, was developed by *Glukhov et al.* [1992]. It relies on a simplified scheme of four constituents, that is, electrons, single positive molecular ions, single negative molecular ions, and positive cluster ions; as well as four different charge exchange processes, those of electron attachment, electron detachment, dissociative recombination, and conversion of molecular positive ions into positive cluster ions. These altitude-dependent processes combine to define the relaxation of electron density enhancements in the D region which are assumed to be responsible for the observed recoveries of early VLF perturbations.

[8] It is important to clarify that the GPI model does not predict the magnitude and/or phase changes evident in the early VLF events. Also it should be noted that, although the present analysis relies on the QE heating mechanism for early VLF event production, the GPI model used here can be applied to any event where ionization is produced at a given level and altitude in the upper D region, no matter what is the exact ionization production mechanism.

[9] The purpose of this work is to introduce a methodology which uses the GPI model to study early VLF event recoveries in order to gain physical insight and obtain estimates of the electron densities produced in the upper D region in association with sprite occurrences. Given that there are no conclusive measurements of TLE-related ionization that scatters VLF waves, such estimates can be a valuable input for existing theoretical models and their implications.

2. Model Formulation

[10] In the following we present details of the GPI model [*Glukhov et al.*, 1992] which are pertinent to the present study. In this model, the electron and ion density changes in the D region can be estimated by taking into account processes affecting the number densities of four kinds of charged particles, that is, electrons, positive ions, negative ions, and positive cluster ions, their number densities denoted as N_e, N^+, N^-, and N_x^+, respectively. The positive ions N^+ include primarily O_2^+ and NO^+, while negative ions N^- may include O_2^-, CO_3^-, NO_2^-, NO_3^-, and others. Positive cluster ions N_x^+ like $H^+(H_2O)_n$ are produced from positive ions N^+ via a hydration chain reaction.

[11] Recently, *Lehtinen and Inan* [2007] extended GPI to include one more constituent, that is, heavy hydrate negative ion clusters N_x^-. This modification becomes important at lower altitudes, e.g., below 50 km, where it can lead to long-lasting ionic conductivity perturbations occurring, for example, in relation with blue jets. *Cotts and Inan* [2007] postulated that this process is likely responsible for unusual cases of long-lasting early event recoveries caused, presumably, by the slowly recombining positive and negative cluster ions below 50 km. For the common early VLF events under study, which occur mostly in relation with sprites and are attributable to electron density elevations in the upper D region, the simplified GPI model is thought to be adequate. Although it is certainly oversimplified as compared to full time-dependent kinetic models that involve a large number of D region chemical and electrochemical reactions [e.g., see *Gordillo-Vázquez*, 2008], we feel the GPI model is a good approximation and offers considerable insight to the phenomenon dealt with in the present study.

[12] The time evolution of each of the four constituents obeys its own continuity equation, which form the following system of ordinary differential equations (ODE):

$$\frac{dN_e}{dt} = Q + \gamma N^- - \beta N_e - \alpha_d N_e N^+ - \alpha_d^c N_e N_x^+ \quad (1)$$

$$\frac{dN^-}{dt} = \beta N_e - \gamma N^- - \alpha_i N^- \left(N^+ + N_x^+\right) \quad (2)$$

$$\frac{dN^+}{dt} = Q - BN^+ - \alpha_d N_e N^+ - \alpha_i N^- N^+ \quad (3)$$

$$\frac{dN_x^+}{dt} = BN^+ - \alpha_d^c N_e N_x^+ - \alpha_i N^- N_x^+. \quad (4)$$

All four equations are interdependent because of the plasma quasi-neutrality, which requires that $N_e + N^- \simeq N^+ + N_x^+$. The positive and negative terms on the right-hand sides of (1)–(4) represent production and loss terms, respectively. Here Q is the electron production term, which is to be detailed shortly. As for the rest of the coefficients, β is the electron attachment rate, γ the electron detachment rate, α_d is the coefficient of dissociative recombination, α_d^c the effective coefficient of recombination of electrons with positive cluster ions, α_i the coefficient of ion-ion recombination (mutual neutralization) for all kinds of positive ions with negative ions, and B is the rate of conversion of positive ions into positive cluster ions.

[13] The effective electron attachment rate β applies to the 3-body attachment process and is given in s^{-1} by *Rowe et al.* [1974] as:

$$\beta = 10^{-31} N_{O_2} N_{N_2} + 1.4 \times 10^{-29} \left(\frac{300}{T}\right) e^{-\frac{600}{T}} N_{O_2}^2. \quad (5)$$

Here, N_{O_2} and N_{N_2} represent the number densities of molecular oxygen and nitrogen expressed in cm^{-3}, whereas T is the electron temperature taking up typical values of about 200 K during nighttime. The attachment rate is a function of altitude ranging from about 20 s^{-1} to 0.02 s^{-1} between 50 and 80 km [e.g., see *Pasko and Inan*, 1994]. It has to be mentioned that in the presence of a strong electric field the attachment is also due to a 2-body dissociative process [see *Lehtinen and Inan*, 2007; *Pasko et al.*, 1997]. This electric field-dependent process can be included in future studies as an extension to the GPI model, although its exclusion here can be tolerated since the present study models the event recovery phase when the energizing electric field is not anymore present.

[14] The effective detachment rate γ is rather uncertain. There exist different rather speculative approaches, e.g., see discussions by *Pasko and Inan* [1994] and *Lehtinen and Inan* [2007], and more references cited therein, which suggest values that range over several orders of magnitude from 10^{-23} N s^{-1} to 10^{-16} N s^{-1}, where N is the total number density of neutrals expressed in cm^{-3}. Following *Pasko and Inan* [1994], the value of γ used here was taken equal to 3×10^{-18} N s^{-1}.

[15] Based on previous studies [e.g., see *Lehtinen and Inan*, 2007], the effective coefficient of dissociative recombination α_d takes values between 10^{-7} and 3×10^{-7} cm^3 s^{-1}, whereas the effective recombination coefficient of electrons with positive cluster ions α_d^c ranges from $\sim 10^{-6}$ to 10^{-5} cm^3 s^{-1}. In the present calculations, the values of 3×10^{-7} cm^3 s^{-1} and 10^{-5} cm^3 s^{-1} were adopted for α_d and α_d^c, respectively, in line also with *Pasko and Inan* [1994]. In the same manner, the effective coefficient of ion-ion recombination processes for all kinds of positive ions with negative ions is taken to be 10^{-7} cm^3 s^{-1}, while the typical value of B, that is, the effective conversion rate of positive ions N^+ into positive cluster ions N_x^+, is assumed equal to 10^{-31} N^2 s^{-1}, in agreement with *Glukhov et al.* [1992, and references therein], as well as *Lehtinen and Inan* [2007].

[16] For early VLF perturbations attributable to sprites, the production term Q refers to the ionization production rate in a weakly ionized plasma, as is the ionosphere, under the action of an electric field. This problem has been dealt with in a series of papers [e.g., see *Tsang et al.*, 1991; *Papadopoulos et al.*, 1993, and references therein]. The electron production term is expressed as $Q = \nu_i N_e$, where ν_i denotes the ionization frequency, that is the number of ionization events per second per electron. Here, it is computed from the following expression of *Papadopoulos et al.* [1993]:

$$\frac{\nu_i}{\nu_{am}} = \left(0.7 + 4.2e^{-2.6\frac{E}{E_k}}\right)\left(\frac{E}{E_k}\right)^2 \exp\left[-4.7\left(\frac{E_k}{E} - 1\right)\right], \quad (6)$$

taken in the limit $\omega \ll \nu_k$, where ω is the angular frequency of the energizing electric field E and ν_k is an effective electron-neutral collision frequency. In this equation, E_k is the air-breakdown electric field, and ν_{am} is the maximum attachment frequency taken from the expression $\nu_{am} = 7.6 \times 10^{-13}$ N_m cm^3/s, where N_m is the concentration of air molecules expressed in cm^{-3}.

[17] Finally, the ionizing time varying electric field used in the calculations represents an lightning related quasi-electrostatic (QE) field, approximated as:

$$E = E_0 \frac{t}{T_{rs}} e^{-t/\tau_{cc}}, \quad (7)$$

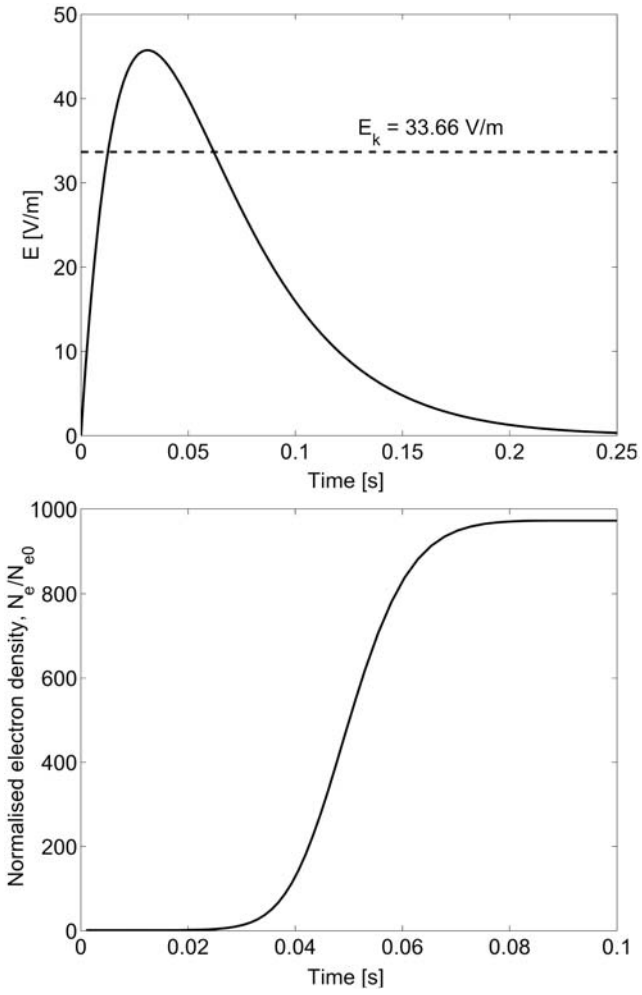

Figure 2. (top) Time response of a lightning-induced QE field impacted on the upper atmosphere and (bottom) the corresponding increase in relative electron density N_e/N_{e0} at 80 km altitude as predicted by the GPI model using equations (6) and (7) to derive the production term. The dashed horizontal line in Figure 2 (top) shows the air-breakdown electric field at 80 km. For a nighttime electron density N_{e0} of $\sim$60 cm^{-3} at 80 km, the elevated electron densities N_e may approach 6×10^4 cm^{-3}.

where T_{rs} and τ_{cc} are characteristic times representing the return stroke and continuing current durations, respectively. Typical values of E_0 are of the order of a few tens of mV/m, of T_{rs} tens of microseconds and of τ_{cc} a few tens of milliseconds. An example of the electric field E pulse at 80 km altitude is shown in Figure 2 (top) where it reaches about 45 V/m, thus exceeding E_k which at this altitude is near 34 V/m. From (7) and Figure 2, we infer that ionization production lasts only for a small fraction of a second. During this time the electrons must have energies of at least a couple of tens of eV in order to exceed the ionization potentials of the main atmospheric constituents, that is, 12.8 eV for O_2 and 15.57 eV for N_2. On the other hand, the electrons taking part in the loss processes must be thermal electrons with energies $\ll$1 eV. Apparently, this is valid because the energized electrons are quickly thermalized through electron-neutral collisions. Since the electron thermalization time is well below 1 s for D region altitudes [e.g., see *Glukhov et al.*, 1992], the electrons are taken to be thermalized instantly as compared to the electron density relaxation times of tens of seconds which define the recoveries of early VLF perturbations.

3. Numerical Results

[18] To model the relaxation of ionization in the D region, an electron density production level was obtained first by solving the ODE system of (1)–(4) for a given altitude, by setting the production term $Q = \nu_i N_e$ where ν_i was computed from (6) after adopting a proper electric field from (7). The ambient number densities entering the ODE (1)–(4), which constitute the initial conditions for solving the equations, were extracted from the altitude profiles provided by *Glukhov et al.* [1992]. The ODE system was solved numerically using a 4th order Runge-Kutta formulation scheme. An example of the electric field used and N_e produced relative to the ambient electron density N_{e0} at the altitude of 80 km are shown in Figure 2. In this numerical procedure, the driving electric field parameters entering (6) were adjusted in order to produce different electron density enhancement levels N_e relative to background N_{e0} through the electron production rate Q. Next, the perturbed values of all species, obtained during production, were used as initial values to solve again the same ODE system by setting this time the production term $Q = 0$. In this way it is possible to model, at different altitudes and for different electron density production levels, the time evolution of the charged particle densities including of course the relaxation of electron density which is of interest here for comparisons with the recoveries of early VLF events.

[19] Given an initial electron density production N_e, its subsequent relaxation is determined by the combined action of electron attachment-detachment, the electron–single ion recombination and the negative-ion and cluster-ion production and recombination processes, all acting under conditions of plasma neutrality. The interplay of these processes can be appreciated in Figures 3 and 4, which show the evolution of the charged species number densities at 75 km (Figures 3 and 4, top), 80 km (Figures 3 and 4, middle), and 85 km (Figures 3 and 4, bottom), for different electron production levels, expressed by the ratio N_e/N_{e0}. The N_{e0} values adopted for the above three heights were 6, 60 and 350 cm^{-3}, respectively, as estimated from an ambient electron density profile used in the paper by *Glukhov et al.* [1992].

[20] Figure 3 illustrates the altitude effects on plasma relaxation for relatively low N_e production levels ($N_e/N_{e0} = 10^2$). At lower heights (Figure 3, top, for 75 km), the decay of N_e and N^+ during the first 50–100 s are nearly symmetric to the growth of N^- and N_x^+, respectively. This suggests that electron attachment, which produces negative molecular ions, and the conversion of N^+ to cluster ions through hydration are the dominant processes. At higher altitudes (see Figure 3, middle and bottom, for 80 and 85 km) the efficiency of these two processes is reduced and so does the relative importance of negative molecular and positive cluster ions. The growth rates of N^- and N_x^+ are much faster at lower altitudes because of their strong dependence on

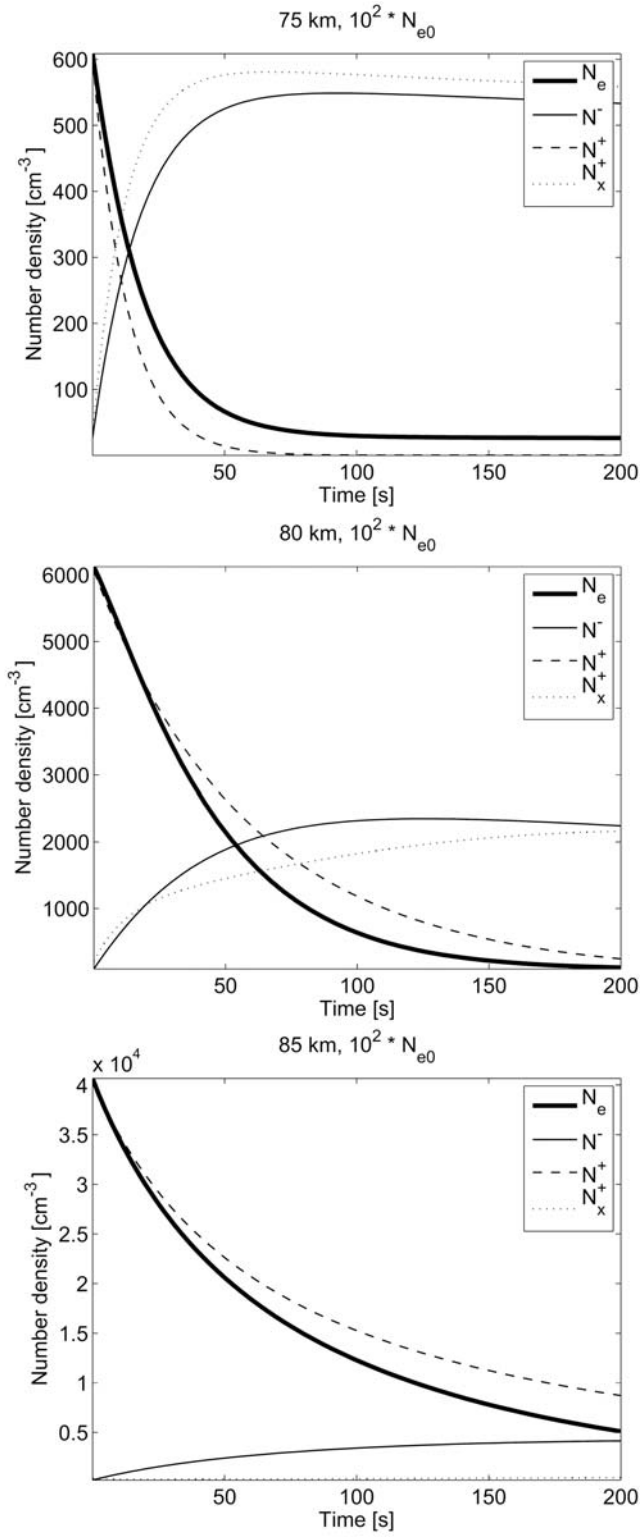

Figure 3. GPI model time evolution of the number densities of all four charged constituents entering the model, for different heights in the upper D region and for a relatively low electron density production ratio $N_e/N_{e0} = 10^2$. (top) For 75 km, (middle) for 80 km, and (bottom) for 85 km. See text for details.

neutral number densities, e.g., see the dependence of the attachment coefficient β in equation (5). On the other hand, the electron–single positive ion dissociative recombination has a limited effect at lower altitudes (say, below 75 km) but gradually becomes the main loss mechanism for the electrons at upper heights (e.g., see Figure 3, middle and bottom). Finally, Figure 3 shows that the electron and single positive ion relaxation times increase with increasing altitude while they remain fast as compared to the slow relaxation of N^- and N_x^+.

[21] The GPI model predicts that for higher N_e production levels the effect of dissociative recombination becomes more decisive in the relaxation of plasma. This is simply because dissociative recombination is nearly proportional to N_e^2 for small number densities of negative molecular and positive cluster ions. This is illustrated in Figure 4 which displays two sets of similar plots as in Figure 3, one for $N_e/N_{e0} = 10^3$ (Figure 4, left) and one for $N_e/N_{e0} = 10^4$ (Figure 4, right). Careful inspection of the curves in Figure 4 shows that dissociative recombination can affect the electron density relaxation significantly. At lower heights, the effect is smaller and is confined during the first stage of relaxation when electron density is highest and N^- and N_x^+ are still small. At upper heights, recombination becomes fairly dominant for larger N_e enhancements, which results to a faster decay of N_e and N^+ and thus shorter relaxation times. For example at 80 km (85 km), the N_e relaxation time is reduced from about 120 s (200 s) to about 75 s (50 s) if N_e/N_{e0} is set to 10^3 (10^4). It is interesting that this dissociative recombination effect on electron density relaxation was not emphasized much in the *Glukhov et al.* [1992] paper.

[22] Since we are interested here in modeling early VLF event recoveries, we display dimensionless values of N_e relative to the ambient electron density N_{e0}, all normalized to their maxima. The model predictions for altitudes ranging from 60 to 85 km are shown in Figure 5. Figure 5 (left) refers to the heights of 60, 65, and 70 km whereas Figure 5 (right) refers to 75, 80, and 85 km (from top to bottom). The curves for each altitude were computed for three initial electron density production levels, corresponding to N_e/N_{e0} ratios equal to 10^2 (dashed lines), 10^3 (dotted), and 10^4 (dash-dotted).

[23] As shown in Figure 5 (left), which refer to altitudes $\leq$70 km, the relaxation times are small and do not depend much on the initial level of electron density. This is because electron attachment is by far the dominant electron loss mechanism at lower heights below about 70 km since it depends strongly on neutral density. The N_e relaxation times, estimated here to be the time required for the electron density to reach the 0.05 level, range from $\sim$1 s at 60 km to $\sim$20 s at 70 km, which are below the measured recoveries for the majority of sprite-related early VLF events [e.g., see *Mika et al.*, 2006]. Inspection of the relaxation curves in Figure 5 (right) for higher altitudes, that is, for 75, 80, and 85 km, shows that the electron density production level has now a clearly discernible effect on the overall electron loss term. As mentioned, this effect increases toward higher altitudes as the electron–single positive ion recombination loss mechanism becomes increasingly important.

[24] Figure 6 summarizes the estimated electron density relaxation time as a function of altitude and N_e/N_{e0} produc-

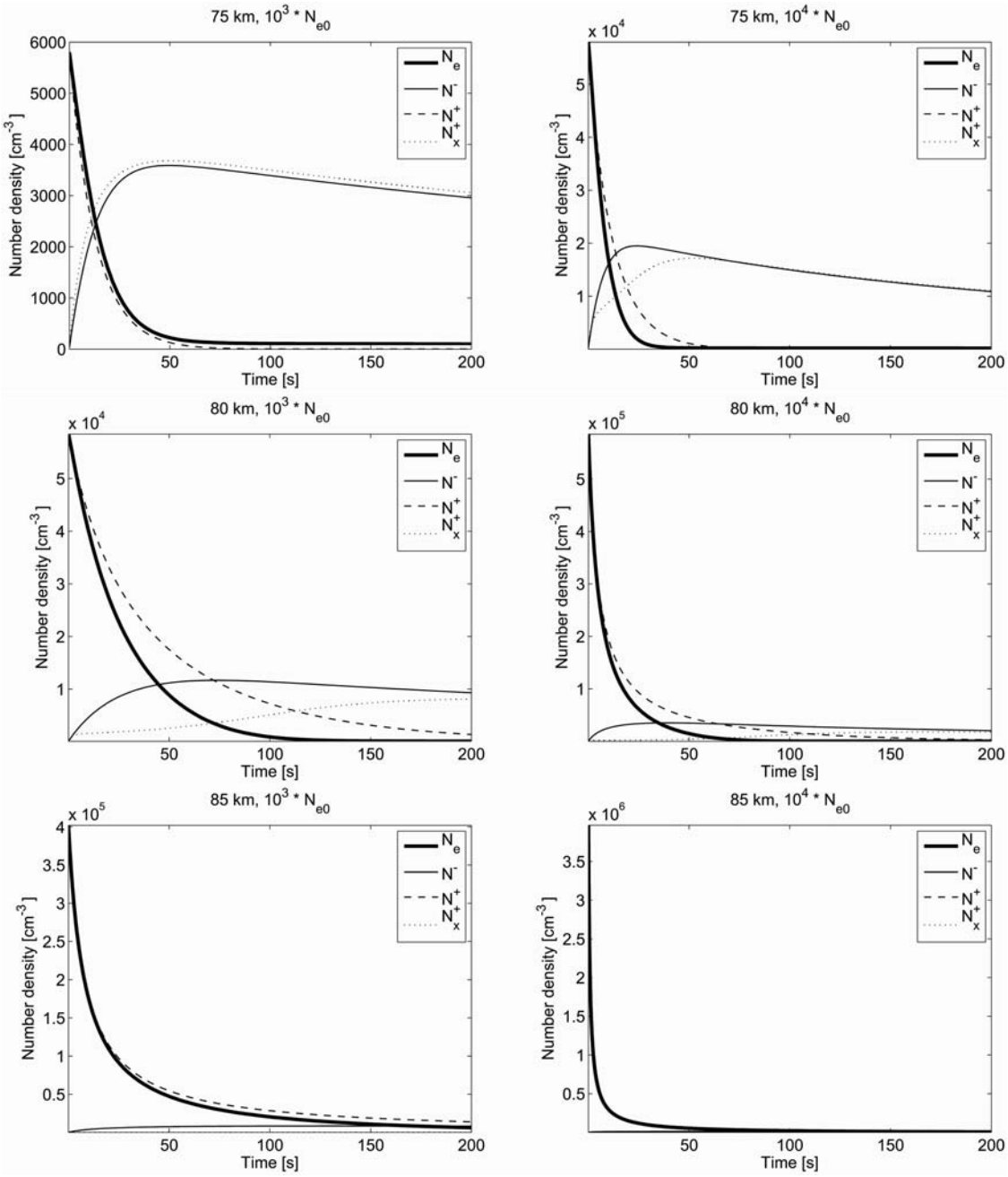

Figure 4. Same as in Figure 3 but for higher electron density production ratios relative to background. (left) $N_e/N_{e0} = 10^3$ and (right) $N_e/N_{e0} = 10^4$.

tion ratio, obtained by curve-fitting approximate relaxation times deduced from Figure 5. As seen, short relaxation times, say <30 s, tend to associate with lower altitudes and appear to be insensitive to the initial level of ionization production relative to the background density. On the other hand, relatively large relaxation times are biased toward upper D region heights and lower N_e/N_{e0} ratios. This results because at upper D region heights the number of single (molecular) positive ions N^+ approaches that of electrons in the quasi-neutrality condition because negative and cluster ion densities drop rapidly above about 75 km to 80 km. As seen, the range of relaxation times with altitude depends critically on N_e/N_{e0}, whereas at a given altitude the larger recovery values correspond to lower N_e/N_{e0} ratios. Further inspection of Figure 4 shows that for a given N_e/N_{e0} ratio, the relaxation time increases with altitude at a rate that is larger for lower N_e/N_{e0} ratios, apparently because dissociative recombination is now slower because it depends approximately on N_e^2.

[25] Based on the above discussion, and given that the recoveries of sprite-associated early VLF events range between about 20 and 250 s [e.g., *Mika et al.*, 2006], we postulate that the regions of electron density enhancements responsible for most of the early events are situated between ~70 km and the VLF reflection heights nearing 85 to 90 km. This will be illustrated by considering typical early VLF

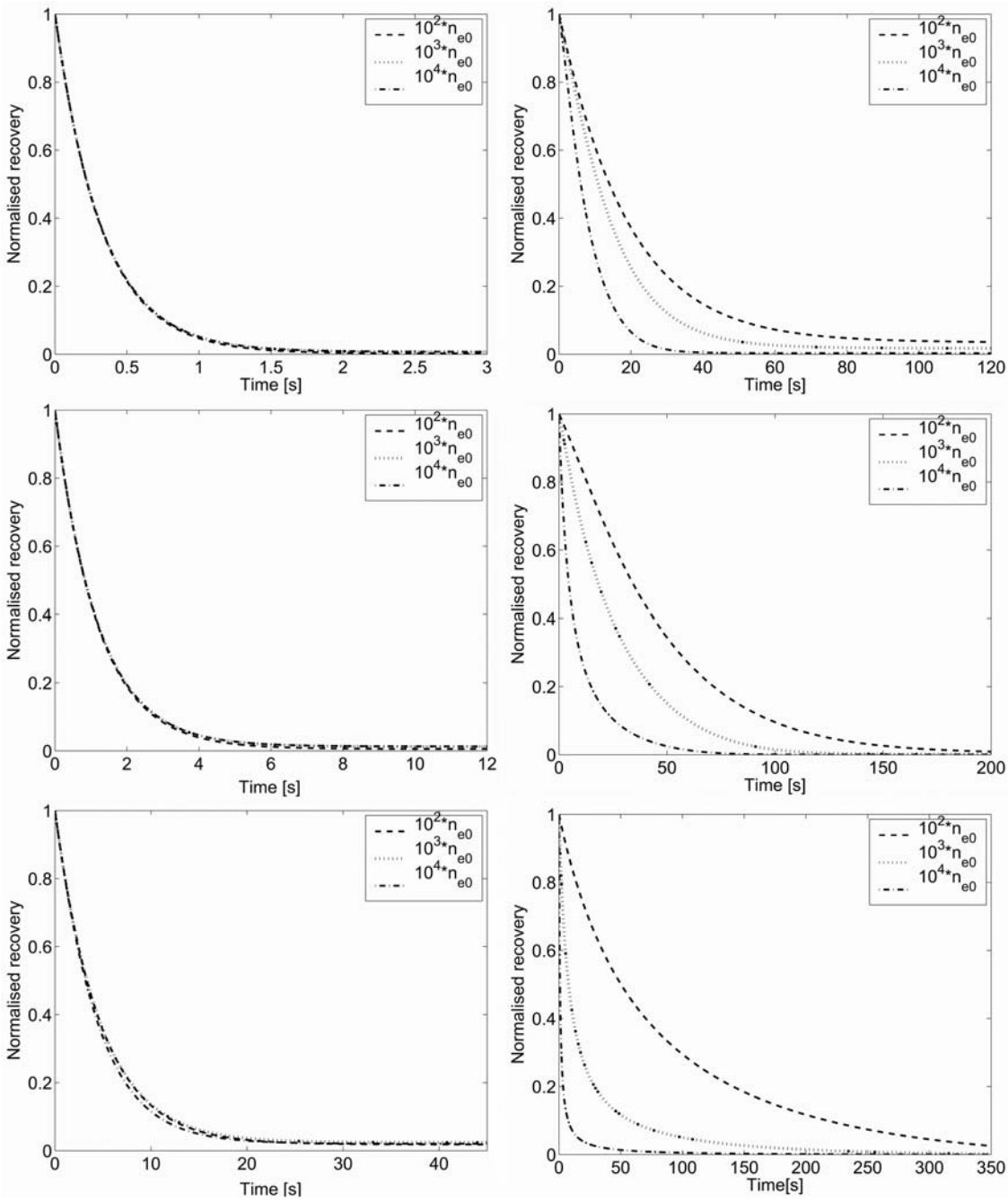

Figure 5. GPI model electron density relaxation curves at (left) 60, 65, and 70 km and at (right) 75, 80, and 85 km (from top to bottom), all normalized at their maximum values. The relaxation curves in each plot correspond to three different electron density production levels, low ($N_e/N_{e0} = 10^2$), medium ($N_e/N_{e0} = 10^3$), and high ($N_e/N_{e0} = 10^4$). Note that the timescales differ in order for the differences between the curves shown in each plot to be discerned.

events and compare their recoveries with those estimated by the present model.

4. Comparison With Data

[26] Early VLF perturbation recoveries observed in association with sprites are compared qualitatively with electron density relaxation times predicted by the GPI model. This serves as a test of the model's suitability while it allows one to obtain approximate estimates of elevated electron densities in the upper D region. Here typical examples of early VLF events are considered, selected from observations made in the 2003 EuroSprite campaign [e.g., *Neubert et al.*, 2005], to be representative of short (~30 s), medium (~100 s), and long (~250 s) early event recovery times. To do approximate comparisons, the VLF signal amplitude recoveries were normalized to their maximum and then superimposed on model predictions of electron density

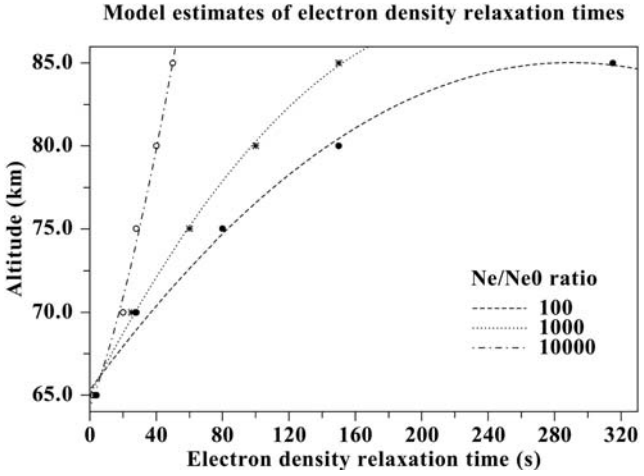

Figure 6. Model estimates of electron density relaxation time (indicated by the symbols) and curves fitted to them, shown as a function of altitude for different N_e/N_{e0} ratios of elevated electron density relative to ambient nighttime values. As seen, the larger relaxation times correspond to higher altitudes and to lower N_e/N_{e0} ratios. Small relaxation times tend to occur at lower altitudes where they are less sensitive to the N_e/N_{e0} production level.

relaxation curves similar to those shown in Figure 5 for the altitudes of 75, 80, and 85 km and initial electron density production levels of N_e equal to 10^2, 10^3, and 10^4 times that of the ambient level N_{e0}.

[27] The results are summarized in Figure 7. Figure 7 (top, middle, and bottom) refers to different early VLF events, with Figure 7 (top) corresponding to the event with the shortest recovery time (~30 s) and Figure 7 (bottom) with the longest one (~250 s). Figure 7 (left, middle, and right) refers to different initial relative electron density production levels N_e/N_{e0}, that is, 10^2 for Figure 7 (left), 10^3 for Figure 7 (middle), and 10^4 for Figure 7 (right). The model outputs for 75, 80, and 85 km altitudes are shown in each plot by the dashed, dotted, and dash-dotted electron relaxation curves, respectively. The timescales of the plots are different in Figure 7 (left, middle, and right) in order to facilitate comparisons. As seen, the shape of the observed early VLF amplitude recoveries resemble the simulated ones quite well; both have been characterized by similar time dependencies. Inspection of Figure 7 (top, middle, and bottom) leads to the following inferences:

[28] 1. Early VLF events with short recoveries (<30 s) can be accounted for by considering large sprite-produced electron density enhancements relative to background values to be located preferentially at lower altitudes, say at about 75 km. In this case, the initial electron density enhancements need to reach relatively high levels, up to $\sim 10^4$ times the undisturbed electron densities. Using at 75 km an ambient nighttime electron density of ~6 electrons per cm^3 ($N_{e0} \sim 6$ cm^{-3}), the model estimates an elevated electron density of about 6×10^4 cm^{-3}.

[29] 2. Early VLF events with medium recovery times around 100 s can be modeled by considering elevated electron densities which are now located higher up, say ~80 km, having initial electron density enhancements of 10^3 times N_{e0}. Using here an ambient nighttime electron density of ~60 cm^{-3} at 80 km, the elevated electron density in the affected region may approach 6×10^4 cm^{-3}.

[30] 3. Long-recovery early VLF events, that is, recovery times as high as 250 s, can be accounted for by considering comparatively lower N_e enhancements relative to background, at upper D region altitudes near the VLF reflection heights. By taking at 85 km an ambient nighttime electron density $N_{e0} \sim 350$ cm^{-3}, the model estimates an elevated electron density near 3.5×10^4 cm^{-3} to be responsible for the long recovery of the VLF events.

[31] These inferences can be understood by considering the increased importance with altitude of the electron–single (molecular) ion recombination process. Also at lower heights, one needs to consider the roles of electron attachment and detachment as well as the negative and cluster ion production and recombination processes. Based on the GPI model and the discussion in the previous sections, we conclude that, although electron attachment and cluster ion production play an important role at lower heights, the key process for the recoveries of sprite-related early VLF events in the 75 to 85 km altitude range is electron–molecular ion recombination under approximate $N_e \sim N^+$ plasma-neutrality conditions.

5. Discussion and Concluding Comments

[32] By taking into account the role of electron–single ion dissociative recombination in the upper D region and the conductivity shielding effects of the energizing electric fields inside sprite discharges, a simplified interpretation can be outlined as follows. Relatively strong electric fields are expected to exceed the air-breakdown threshold at lower D region heights and produce large levels of ionization relative to background without significantly affecting higher altitudes because the increased conductivity will enhance shielding effects. In this case, an early VLF event will have shorter recoveries not only because electron attachment and cluster ion production is much more effective at lower heights than at higher, but also because electron–single ion recombination losses increase for higher electron density production levels. On the other hand, a weaker electric field could penetrate higher up into the D region where it may exceed the air-breakdown field to produce lower ionization levels relative to background than in the previous case. This can cause an early VLF perturbation which now, however, will be lasting longer because electron density recovery is slower. This is because electron attachment and cluster ion production at upper heights is much less important compared to the electron–single ion dissociative recombination process. The latter, which is now the dominant electron loss mechanism, depends on $\sim N_e^2$ at upper D region heights and thus becomes slower for lower electron density production levels.

[33] The absolute electron density enhancement estimates responsible for early VLF events, inferred from comparisons of model predictions with measured event recoveries, are found to be higher than 10^4 electrons per cm^3. These estimates of course need to be taken as tentative since they depend on background (ambient) D region electron density, which may vary considerably from night to night. In this respect, the values quoted above are likely to be rather high

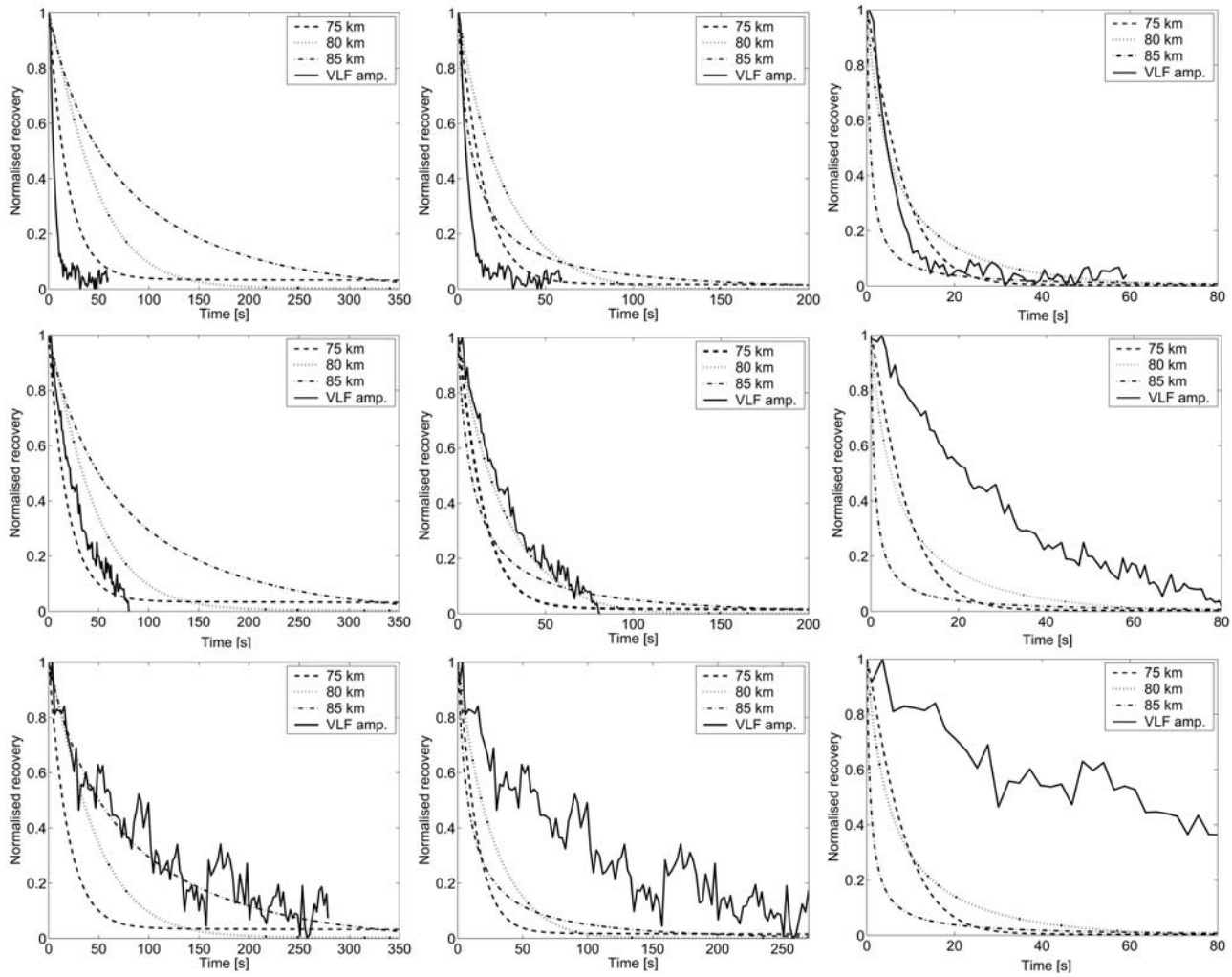

Figure 7. Approximate GPI model fits of EuroSprite-observed VLF perturbation recoveries; all occurred in relation with sprites. Figure 7 (top, middle, and bottom) corresponds to different events, representing (top) short, (middle) medium, and (bottom) long-recovery durations of about ~30 s, ~100 s, and ~250 s, respectively. (left) An electron density elevated $100 \times N_{e0}$, (middle) $1000 \times N_{e0}$, and (right) $10000 \times N_{e0}$. Dashed lines mark curves calculated at 75 km, dotted lines mark those at 80 km, and dash-dotted lines mark those at 85 km. The solid lines correspond to observations of early VLF event recoveries.

because they had been based on a rather elevated D region ambient electron density profile, that was adopted from *Glukhov et al.* [1992]. Likely, the obtained electron density estimates would have been lower if lower ambient electron densities are used, for example in line with the observations of *Cheng et al.* [2006].

[34] Conclusive measurements of sprite-related ionization in the upper D region are in general unavailable in order to be used for comparisons. On the other hand, the values inferred here are higher when compared to existing theoretical estimates. For example, the simulations of *Pasko et al.* [1995, 1997, 1998] for direct QE field heating and ionization predict during sprite discharges electron densities of about 10^3 cm^{-3} inside diffuse sprite glow regions at altitudes above ~70 km. Also, the simulations of *Moore et al.* [2003], which dealt with early VLF events produced by electron density changes associated with sprite halos, invoked electron density enhancements less than 10^3 cm^{-3} in order to reproduce moderate early VLF amplitude changes <0.8 dB.

[35] Alternatively, the possibility exists that the relatively high electron density estimates inferred in the present study are representative of ionization inside an assembly of sprite streamers which intrude into upper D region heights from below or a set of downward sprite streamers which initiate at upper D region altitudes, possibly as high as 90 km. Actually, this option is supported by recent triangulated sprite observations obtained simultaneously with multiple, high-resolution and high-sensitivity cameras, as discussed by *Srenbaek-Nielsen et al.* [2009] during the recent Penn State University Chapman conference. Rationally, it is much easier to get high electron densities in localized regions where streamers propagate, rather than filling large volumes in space with high electron densities (V. P. Pasko, private communication). Then, and from the point of view of electro-chemical relaxation, it may be possible that the

VLF scattering, from a superposition of a large number of streamers spread over an extended region, measures primarily the decay of plasma inside the streamers which, presumably, are rather dense initially (V. P. Pasko, private communication). Unfortunately, the optical sprite images accompanying the early VLF events examined in the present study did not provide information on the altitude of sprite formations; also they did not provide conclusive evidence on upper D region streamer structures and sprite diffuse glows and/or sprite halos, apparently because the cameras used in early EuroSprite campaigns were not very sensitive and of limited time resolution (20 ms). We feel that the question as to what part of the sprite discharge and ionization is responsible for the concurrently observed early VLF events remains open at present and is an important topic that requires more study.

[36] In conclusion, it has been shown that the recoveries of early VLF events, which are observed concurrently with sprites, can be simulated reasonably well by the GPI [*Glukhov et al.*, 1992] relaxation model. The methodology applied here relies on the postulation that most of early VLF events are due to scattering from electron density enhancements located in the upper D region ionosphere between about 70 and 90 km. The early VLF recoveries then are determined mainly by the level of the produced electron density relative to background and the dissociative electron–single ion recombination process. The postulations adopted in the present study led to the conviction that early VLF events with relatively short recoveries may come from lower heights during large elevations in electron density production relative to ambient values. On the other hand, early VLF events with long recoveries may associate with relatively weakly ionized regions relative to background at higher altitudes near the VLF reflection heights where electron–single ion dissociative recombination becomes the dominant loss mechanism. Finally, the comparisons of the model results with observed typical early event recoveries led to tentative estimates of electron density elevations reaching values possibly higher than 10^4 electrons per cm^3 inside the altitude range from about 70 to 85 km. Although the GPI model methodology applied here for the investigation of early VLF events needs more development and testing, it is promising for a better physical understanding and useful in deducing ionization estimates in the upper D region during sprite occurrences.

[37] **Acknowledgments.** We are grateful to Umran Inan of Stanford University and Torsten Neubert of the Danish Space Center for their continuous encouragement and support of the VLF sprite studies at the University of Crete. One of the authors (C.H.) wishes to thank Victor Pasko of Pennsylvania State University for several fruitful discussions during the 2009 PSU Chapman conference.

[38] Wolfgang Baumjohann thanks Francisco Gordillo-Vázquez and another reviewer for their assistance in evaluating this paper.

References

Barrington-Leigh, C. P., U. S. Inan, and M. Stanley (2001), Identification of sprites and elves with intensified video and broadband array photometry, *J. Geophys. Res.*, *106*, 1741.

Cheng, Z., S. A. Cummer, D. N. Baker, and S. G. Kanekal (2006), Nighttime D region electron density profiles and variabilities from broadband measurements using VLF radio emmisions from lightning, *J. Geophys. Res.*, *111*, A05302, doi:10.1029/2005JA011308.

Cotts, B. R. T., and U. S. Inan (2007), VLF observation of long ionospheric recovery events, *Geophys. Res. Lett.*, *34*, L14809, doi:10.1029/2007GL030094.

Cummer, S. A., and W. A. Lyons (2005), Implications of lightning charge moment changes for sprite initiation, *J. Geophys. Res.*, *110*, A04304, doi:10.1029/2004JA010812.

Dowden, R. L., J. B. Brundell, W. A. Lyons, and T. Nelson (1996), Detection and location of red sprites by VLF scattering of subionospheric transmissions, *Geophys. Res. Lett.*, *23*(14), 1737–1740.

Gerken, E. A., and U. S. Inan (2000), Observations of decameter scale morphologies in sprites, *J. Atmos. Sol. Terr. Phys.*, *65*, 567–572.

Glukhov, V., V. Pasko, and U. Inan (1992), Relaxation of transient lower ionospheric disturbances caused by lightning-whistler-induced electron precipitation, *J. Geophys. Res.*, *97*, 16,951–16,979.

Gordillo-Vázquez, F. J. (2008), Air plasma kinetics under the influence of sprites, *J. Phys. D Appl. Phys.*, *41*, 234016, doi:101088/0022-3727/41/23/234016.

Haldoupis, C., T. Neubert, U. S. Inan, A. Mika, T. H. Allin, and R. A. Marshall (2004), Subionospheric early VLF signal perturbations observed in one-to-one association with sprites, *J. Geophys. Res.*, *109*, A10303, doi:10.1029/2004JA010651.

Haldoupis, C., R. J. Steiner, A. Mika, S. Shalimov, R. A. Marshall, U. S. Inan, T. Bosinger, and T. Neubert (2006), "Early/slow" events: A new category of VLF perturbations observed in relation with sprites, *J. Geophys. Res.*, *111*, A11321, doi:10.1029/2006JA011960.

Inan, U. S., and D. L. Carpenter (1987), Lightning-induced electron precipitation events observed at L $\sim$ 2.4 as phase and amplitude perturbations on subionospheric VLF signals, *J. Geophys. Res.*, *92*, 3293–3303.

Inan, U. S., T. F. Bell, V. P. Pasko, D. D. Sentman, E. M. Wescott, and W. A. Lyons (1995), VLF signatures of ionospheric disturbances associated with sprites, *Geophys. Res. Lett.*, *22*, 3461.

Johnson, M. P., and U. S. Inan (2000), Sferic clusters associated with early/fast VLF events, *Geophys. Res. Lett.*, *27*, 1391–1394.

Johnson, M. P., U. S. Inan, and S. J. Lev-Tov (1999), Scattering pattern of lightning-induced ionospheric disturbances associated with sprites, *Geophys. Res. Lett.*, *26*, 12,363.

Lehtinen, N. G., and U. S. Inan (2007), Possible persistent ionization caused by giant blue jets, *Geophys. Res. Lett.*, *34*, L08804, doi:10.1029/2006GL029051.

Marshall, R. A., U. S. Inan, and W. A. Lyons (2006), On the association of early/fast very low frequency perturbations with sprites and rare examples of VLF backscatter, *J. Geophys. Res.*, *111*, D19108, doi:10.1029/2006JD007219.

Marshall, R. A., U. S. Inan, and T. W. Chevalier (2008), Early VLF perturbations caused by lightning EMP-driven dissociative attachement, *Geophys. Res. Lett.*, *35*, L21807, doi:10.1029/2008GL035358.

Mika, A., and C. Haldoupis (2008), VLF studies during TLE observations in Europe: A summary of new findings, *Space Sci. Rev.*, *137*, 489–510, doi:10.1007/s11214-008-9382-8.

Mika, A., C. Haldoupis, R. A. Marshall, T. Neubert, and U. S. Inan (2005), Subionospheric VLF signature and their association with sprites observed during EuroSprite 2003, *J. Atmos. Sol. Terr. Phys.*, *67*, 1580–1597.

Mika, A., C. Haldoupis, T. Neubert, H. T. Su, R. R. Hsu, R. Steiner, and R. A. Marshall (2006), Early VLF perturbations observed in association with elves, *Ann. Geophys.*, *24*, 2179–2189.

Moore, C. R., C. P. Barrington-Leigh, U. S. Inan, and T. F. Bell (2003), Early/fast VLF events produced by electron density changes associated with sprite halos, *J. Geophys. Res.*, *108*(A10), 1363, doi:10.1029/2002JA009816.

Neubert, T., et al. (2005), Co-ordinated observations of transient luminous events during the EuroSprite 2003 campaign, *J. Atmos. Sol. Terr. Phys.*, *67*, 807–820.

Papadopoulos, K., G. Milikh, A. Gurevich, A. Drobot, and R. Shanny (1993), Ionization rates for atmospheric and ionospheric breakdown, *J. Geophys. Res.*, *98*, 17,591–17,596.

Pasko, V. P., and U. S. Inan (1994), Recovery signatures of lightning-associated VLF perturbations as a measure of the lower ionosphere, *J. Geophys. Res.*, *99*, 17,523–17,537.

Pasko, V. P., U. S. Inan, Y. N. Taranenko, and T. F. Bell (1995), Heating, ionization and upward discharges in the mesosphere due to intense quasi-electrostatic thundercloud fields, *Geophys. Res. Lett.*, *22*, 365–368.

Pasko, V. P., U. S. Inan, T. F. Bell, and Y. N. Tararenko (1997), Sprites produced by quasi-electrostatic heating and ionization in the lower ionosphere, *J. Geophys. Res.*, *102*, 4529–4561.

Pasko, V. P., U. S. Inan, and T. F. Bell (1998), Spatial structure of sprites, *Geophys. Res. Lett.*, *25*, 2123–2126.

Peter, W. B., and U. S. Inan (2005), Electron precipitation events driven by lightning in hurricanes, *J. Geophys. Res.*, *110*, A05305, doi:10.1029/2004JA010899.

Poulsen, W. L., T. F. Bell, and U. S. Inan (1993), The scattering of VLF waves by localized ionospheric disturbances produced by lightning-induced electron precipitation, *J. Geophys. Res.*, *98*, 15,553–15,559.

Rodger, C. J. (2003), Subionospheric VLF perturbations associated with lightning discharges, *J. Atmos. Sol. Terr. Phys.*, *65*, 591–606.

Rowe, J. N., A. P. Mitra, A. J. Ferraro, and H. S. Lee (1974), An experimental and theoretical study of the D-region-II. A semi-empirical model for mid-latitude D region, *J. Atmos. Terr. Phys.*, *36*, 755.

Srenbaek-Nielsen, H. C., R. Haaland, M. G. McHarg, T. Kanmae, and B. A. Hensley (2009), Sprite initiation altitude measured by triangulation, paper presented at Chapman Conference on the Effects of Thunderstorms and Lightning in the Upper Atmosphere, Am. Geophys. Union, Pa. State Univ., University Park, 10–14 May.

Tsang, K., K. Papadopoulos, A. Drobot, P. Vitello, P. Wallace, and R. Shanny (1991), RF ionization of the lower ionosphere, *Radio Sci.*, *26*, 1345–1360.

Voss, H. D., et al. (1984), Lightning induced electron precipitation, *Nature*, *312*(5996), 740–742.

C. Haldoupis, Physics Department, University of Crete, Heraklion, GR-71003 Crete, Greece. (chald@physics.uoc.gr)

Á. Mika, BMT ARGOSS B.V., Voorsterweg 28, NL-8316 PT Marknesse, Netherlands. (agnes.mika@bmtargoss.com)

S. Shalimov, Institute of Physics of the Earth, B. Grunzinskaiya 10, 123810 Moscow, Russia. (pmsk7@mail.ru)